Nanoscale craters in poly(methyl methacrylate) formed by exposure to condensing solvent vapor

Student:	Christopher M. Bates
Presentation Semester:	Spring – 2008
Advisor	J. Thomas Dickinson
Department:	Physics and Astronomy
College:	College of Sciences

Précis

The microscopic structure of a surface can affect many of its properties: washing, painting, coating, and even adhesion. These alterations in properties can arise solely from physical changes to the surface of the material. For example, a tree frog adheres to a surface not from a glue-like substance or a mucous membrane but solely from the micron-sized structures on its toes pads. Also, small projections on the leaves of the lotus flower keep water droplets suspended above the surface of the leaf which, upon falling off, carry dust and other particles with it. For these reasons I was very interested to find a project to study submicron structure formation, which became a study of the formation of nanometer and micrometer diameter craters.

In order to analyze submicron crater formation I needed a way to form, image, and assess these modifications. Reading a paper by Bonaccurso et al.[7] gave me the idea of using a polymer surface with ink-jet deposited drops of solvent. The only problem was that these ink-jet deposited droplets were roughly 20 μm in diameter at smallest, which was approximately 20 times larger than desirable. To overcome this we came up with the idea to use a higher surface tension solvent, which would give a higher volume-to-contact-area ratio, a smooth polymer substrate, and solvent vapor condensation, which made the largest difference. To image the resulting features we used an atomic force microscope, which runs a cantilever over a surface and basically outputs the physical deflections into images. This physical method of imaging was not a problem due to the robustness of these features.

Later, we were faced with a problem. Pits were forming, but their depth-to-diameter ratios were too small, i.e. the pits were too wide and shallow. We wondered how to obtain a higher volume-to-contact-area ratio for the droplets and came upon a way to increase the surface

tension of the solvent. The subsequent addition of ammonia vapor to the droplets results in ions forming in the condensing solvent drops. This electrolyte formation increases the surface tension of the drop, thereby increasing the solvent volume-to-contact-area ratio we needed to achieve.

To better quantify our results we wrote a program that would analyze the net volume change associated with these craters. To our surprise the formation of these craters was associated with a net negative volume change; inconsistent with other solvent drop on polymer experiments. We tested a number of hypotheses until we did experiments that supported a local increase in density and hardness, which was consistent with the volume change observed.

All of our experiments showed that micron- and nanometer diameter pits can be produced on our polymer surface using our new condensing solvent vapor technique. This new technique allows for much more efficient coverage of the surface, smaller pit diameters, and higher depth-to-diameter ratios relative to previously reported pits, with the downside of randomized pit location. The significance of this study is that we have been able to characterize a system for creating reproducing nanometer scale pitted surfaces, which can have profound effects on the physical properties of the polymer.

The next step in this research would be to experiment with the applications of these surfaces. As a template these surfaces could be used to create self-adhesive strips of polymer that adhere solely due to their physical structure. There is also a possibility for a self cleaning surface, which could be very useful. There are current nanolithographic techniques that can achieve these surfaces but they are much more costly and time consuming compared to our solvent vapor condensation technique.

Table of Contents

Nanoscale craters in poly(methyl methacrylate) formed by exposure to condensing solvent vapor

C.M. Bates

Physics Department, Washington State University, Pullman, Washington 99164-2814

I. INTRODUCTION

The controlled formation of submicron pits plays an important role in several important technologies. Small pits can be used as nanovessels, which are tiny reactors for microchemistry and nanochemistry. Nanovessels not only minimize reactant volume, but also dissipate heat efficiently due to their high surface area-to-volume ratio. On submicron scales, diffusion is especially rapid, potentially significantly reducing the time required for a reaction to proceed to completion. Pits that extend completely through a film can serve as pathways for controlled transport. Arrays of pits can also be used as templates for the casting of microlens arrays, which have potential applications in data transmission, copy machines, and laser printers.[1] Sub-micrometer patterning can also affect important surface properties for washing, printing, painting, and coating.[2–5] For instance, the structured surfaces of tree frog toe pads provide adhesion on near-vertical surfaces.[6]

Pits can be formed on polymer surfaces by drops of volatile solvents.[7–10] Using an ink-jet system to deposit drops of toluene on polystyrene, Bonaccurso et al.[7] produced patterns of pits as small as 20 μm in diameter, with aspect ratios (depth-to-diameter ratios) as high as 0.1. In this

system, pit formation was attributed to the "coffee stain effect," where polymer dissolved near the center of the drop is transported to the perimeter and deposited as the solvent evaporates. (A similar process produces ring-like stains when coffee is spilled on a hard surface.[4])

In this work, we characterize pits formed on poly(methyl methacrylate) (PMMA) films by the condensation of small acid drops from formic acid vapor. Formic acid is a strong solvent for PMMA and has a high vapor pressure at room temperature. In contrast with pit formation in the toluene–polystyrene system,[7] formic acid drops produce pits on PMMA primarily by densifying the surrounding polymer. Under these conditions, pit formation is strongly affected by the kinetics of drop growth and coalescence, and can be modified by exposing the polymer film to ammonia vapor immediately after exposure to formic acid.

Although the pits produced by vapor condensation are distributed randomly, high pit densities are easily achieved. These pits can be much smaller than those produced by direct solvent-deposition technologies; less than 50 nm in diameter. Further, significantly higher aspect ratios can be obtained, with depth-to-diameter ratios as high as 0.5. Similar pits may have significant effects on polymer surface properties, including wetability, adhesion, and friction.

II. HYPOTHESIS

Through the controlled exposure of a polymer substrate to condensing solvent vapor, submicron crater formation should be achievable, which would represent vast improvements over previous methods in size, quantity, and depth-to-diameter ratios.

III. MATERIALS AND METHODS

A. Film preparation

Polymer films were cast from a 15% by weight solution of PMMA (Aldrich, St. Louis, MO; MW ≈ 145,000 atomic mass units) in a mixture of 67% propylene glycol methyl ether acetate and 33% γ-butyrolactone. A few drops of polymer solution were placed on a glass microscope slide (Precleaned Gold Seal Micro Slides; Becton Dickinson, and Company), spun at 500–1000 rpm for 10–30 s, and baked at 95 °C for 1 h. The resulting films were 5–15 μm thick. The deposited films had root-mean square roughnesses of approximately 0.3 nm over 3×3 μm^2 areas.

B. PMMA film treatment

Formic acid solutions were prepared from purum grade (≥98%; Fluka) or reagent grade (88%; J.T. Baker) solutions; some solutions were diluted with deionized water. Formic acid drops were condensed onto a PMMA-coated glass slide by holding a slide (PMMA side down) over a 400-mL beaker containing 20 mL of warm formic acid. The solution temperature was controlled with a 300-mL water bath; the reported temperature is that of the bath. Some slides were then immediately exposed to ammonia vapor by holding the slide over a 400-mL beaker containing room-temperature ammonium hydroxide (reagent grade, 28%–30%, J.T. Baker). As we discuss below, the ammonia exposure has a strong influence on the resulting pit morphology. The slides were then removed, allowed to dry, and imaged by atomic force microscopy (AFM). Macroscopic formic acid droplets (<1 mm in diameter) show contact angles ranging from 19° to 25° on our PMMA films, with no discernable difference between 98% and 88% solutions.

C. Pit characterization

The resulting pits were imaged with a Molecular Imaging PicoScan atomic force microscope using square-pyramidal tips with tip angles of 70° ± 4° and nominal radii with a curvature of 20 nm (maximum curvature 60 nm). The nominal cantilever-force constants were between 0.06 and 0.58 N/m. Nanoindentation was performed with a Hysitron Triboscope equipped with a Nanoinstruments Nanoindenter II, using a three-sided pyramidal diamond Berkovich tip at loads from 25 to 400 μN and loading rates between 2.5 and 40 μN/s.

The dimensions of selected pits were calculated from selected AFM data with a Mathematica program. The program determined the deviation of each pixel from the elevation of the surrounding surface and summed the volume (deviation × pixel area) associated with pixels above the surrounding surface; the volume associated with pixels below the surrounding surface was summed independently. The difference between these two volumes corresponds to the net volume change associated with the pit. Pit diameters, depths, average heights, average depths, and average diameters were also determined.

IV a. RESULTS

A. Pit morphologies

Exposing the PMMA films to hot formic acid vapor typically produces large numbers of pits, as shown in Fig. 1. The largest pits in Fig. 1 are about 1 μm in diameter. Much smaller pits also appear (e.g., 50 nm in diameter). By way of comparison, the smallest pits produced by ink-

jet technology are about 20 μm in diameter[7] and would barely fit in Fig. 1. Images acquired almost 1 year after preparation show pits with similar depths, diameters, and aspect ratios as images of the same film acquired hours after preparation. These features are quite robust.

Although the pits persist unchanged for long times at room temperature, annealing pitted films for 2 h at the glass-transition temperature (T_g; near 120 °C) renders them less distinct. Annealing the films for 2 h at 140 °C restores pitted films to their original smooth surfaces. Exposing the smooth films produced by the high-temperature anneal to formic acid vapor again produces pits similar to those produced before the high-temperature anneal. This suggests that pit formation involves the reversible rearrangement of polymer material and not irreversible material removable by volatilization or decomposition.

Some treatments produce pits with unusually large aspect ratios (pit depth-to-diameter ratios). Figure 2 shows an AFM image of a pit formed by exposing a PMMA film to 70 °C, 98% formic acid for 3 s followed by immediate exposure to ammonia vapor. The aspect ratio of this pit is approximately 0.33, about three times the maximum obtained with ink-jet technologies. Like many of the pits seen in Fig. 1, the pit in Fig. 2 displays a raised rim. In contrast with pits formed by direct solvent deposition,[7] the volume of material deposited along the rim of the pit in Fig. 2 is much less than the volume removed from the center. Only 25% of the pit volume can be accounted for by presence of the rim. The remaining 75% of the pit volume represents a net volume loss. Below, we present evidence that this volume loss is due to an increase in the density of the polymer surrounding the pit.

When water vapor condenses in a dropwise fashion on hydrophilic surfaces, the size distribution of the first generation of drops is relatively uniform.[11–13] Significant dispersion in

drop size develops only after the drops are large enough to touch and coalesce. Coalescence generates larger drops while creating surrounding open space for new drops to nucleate. Figure 3 shows a large pit that presumably formed when several small drops condensed to form a large drop. Interestingly, relatively few small pits are observed within 1 μm of the large pit. Studies of drop nucleation and growth show that both processes can be hindered near large drops,[14,15] where the net flux of vapor to the large drop lowers the partial pressure of vapor in the surrounding atmosphere.

Many of the pits formed by exposure to formic acid vapor have smooth, rounded bottoms, like the pit in Fig. 2. Smooth, rounded bottoms are observed on pits of almost any diameter and depth. However, large-diameter pits often display a raised bump in the center, including the largest pit in Fig. 3. Pits with center bumps were typically 2–8 μm in diameter and 20–200 nm in depth, with aspect ratios less than 1:10. Somewhat larger bumps have been produced within pits by ink-jet deposition of solvent mixtures on polystyrene[10]; again, the diameter of these structures was typically much more than a few hundred microns, which is much larger than the structures produced by solvent condensation here.

Drop coalescence occasionally produces more complex pits, ranging from the complex, flower-like pit of Fig. 4(a) to the simple double-pit of Fig. 4(b). While drop coalescence typically produces one large, circular drop, as in Fig. 3, coalescence is not always complete. In Figs. 4(a) and 4(b), the perimeters of the coalescing drops have been pinned. Although the drops touch, the resulting partial coalescence produces complex features.

Formic-acid-treated films often show high densities of smaller, shallow pits. Representative pits in Fig. 4(c) are on the order of 200 nm in diameter and 2 nm deep. Similar

pits appear between the larger features in Figs. 4(a) and 4(b). Careful adjustment of vapor flux, duration, and substrate and vapor temperatures would permit considerable control over the size distribution of the resulting pits.

B. Pit volumes

The net volume change (raised volume minus lowered volume) for a large number of isolated pits produced under a variety of exposure conditions is plotted as a function of pit diameter in Fig. 5. Although some pits display net positive volume changes, over 70% of the analyzed pits show net negative volume changes. In most cases, larger pits are associated with larger (net negative) volume changes.

In principle, volume loss could result from material removal, either by the decomposition and volatilization of near-surface polymer, or by the loss of residual solvent. Since the annealing treatment used to remove the casting solvent used temperatures well below the T_g (95 °C versus $T_g \approx 120$ °C), we cannot rule out the presence of residual solvent. A series of films annealed for 2 h at 140 °C were subsequently treated with formic acid vapor, and displayed pits similar to those observed on films annealed at 95 °C. Residual solvent, if present, has little effect on pit formation. The high-temperature anneal is also expected to increase the polymer density slightly. This density change does not significantly affect pit formation.

To test for mass loss due to polymer decomposition or loss of residual solvent during exposure to formic acid, weighed PMMA films were dissolved in formic acid and the resulting solution was evaporated to dryness. To within the precision of these measurements, the weight of the remaining solid was equal to the initial mass. If the volume loss associated with pit formation

were due to a decrease in polymer mass or to removal of residual solvent, we would expect dissolution and evaporation to yield a measurable mass loss.

Other chemical modifications of the PMMA structure are possible, for instance, hydrolysis of the carbomethoxy side groups. Carbomethoxy group hydrolysis in particular would render the films more hydrophilic and thus decrease the contact angle of water drops on the surface. To probe for this effect, we measured the contact angle of water drops on films cast from the PMMA/formic acid with those on films cast directly from a solution of propylene glycol methyl ether acetate and γ- butyrolactone. These contact angles are equal to within the measurement uncertainties. Although we cannot rule out more subtle effects, formic acid does not react chemically with PMMA under the conditions of this work.

A net volume loss can also be produced by a local increase in polymer density. In this case, one would expect measurable changes in the hardness and elastic modulus. Nanoindentation measurements were performed on a film exposed to 50 °C, 88% formic acid for 10 s with immediate exposure to ammonia vapor. Indents were formed with a load of 400 μN at a loading rate of 40 μN/s. Measurements inside the pits were confined to isolated pits with diameters of at least 3 μm. The average hardness of material inside pits was 0.29 GPa. This is about 50% higher than the average hardness of material outside the pits (0.18 GPa). The average hardness measured outside the pit is virtually identical to the average hardness of untreated films (0.19 GPa). Young's modulus measurements show that the material inside pits is also significantly stiffer than the material outside pits. These results are consistent with the densification of material within the pits.

The mechanical-property measurements rule out the possibility that the pits are formed by the swelling of the surrounding material. AFM measurements of topography cannot distinguish uniform swelling, everywhere except in the pits, from localized volume loss near the pits. Swelling significantly reduces the hardness and modulus of polymer films and this reduction was not observed.

C. Effect of exposure time and acid concentration

A scatter plot of pit diameter versus exposure time over 50 °C, 98% formic acid, without subsequent exposure to ammonia, is shown in Fig. 6. Longer formic acid vapor exposures yield larger drops and thus larger pit diameters, as shown in Fig. 6. Pits formed under these conditions are typically 10–50 nm deep.

The resulting pit depths and shapes are also affected by the concentration of formic acid used to supply the vapor. Fig. 7 shows AFM images of pits on PMMA films exposed to formic acid vapor at 65 °C for 5 s, followed immediately by exposure to ammonia vapor. The small, shallow pits in Fig. 7(a) were formed using 98% formic acid (<2% water). Increasing water concentration to 10% produced deeper pits, which are shown in Fig. 7(b). The smallest pits in Fig. 7(b) have especially high aspect ratios. Increasing water concentration further to 20% produced larger, shallow pits with lower aspect ratios, shown in Fig. 7(c). The highest aspect ratios were observed on films exposed to 90% formic acid solution and then immediately exposed to ammonia vapor. Significantly, the size of the largest pits in Fig. 7 increases as the formic acid concentration is reduced. Hence, small pits prefer more a concentrated solution.

D. Effect of ammonia vapor

A scatter plot of pit depth and diameter measurements for films exposed to 98% formic acid vapor with and without subsequent ammonia exposure is shown in Fig. 8. To provide a range of pit dimensions, the duration of formic acid exposure and the water bath temperature were varied. When a brief exposure to formic acid is immediately followed by room-temperature ammonia vapor, the resulting pits are often significantly deeper; these pits often display significantly higher aspect ratios. The affect of ammonia exposure on pits produced by exposure to 50 °C, 88% formic acid for 10 s is shown in Fig. 9. Under these conditions, ammonia exposure increases the average pit depth by a factor of four, from 22 ± 5 to 95 ± 28 nm.

Naively, one expects the evaporation of a solution containing formic acid and ammonia to form ammonium formate, a crystalline salt. Crystalline residues are observed on PMMA films given high doses of both formic acid and ammonium hydroxide vapor, where high doses of ammonia were provided by heating the ammonium hydroxide as well as the formic acid solution. However, no such deposits are observed following exposure to room-temperature ammonia vapor. We expect that the amount of ammonia incorporated into formic acid drops under these conditions is insufficient to leave a detectable residue. As discussed below, the presence of ammonium ions would increase the electrolyte concentration and thereby increase the surface tension and contact angle.[16] Increasing the contact angle reduces the diameter and increases the height of formic acid drops, thereby increasing the depth of the affected polymer beneath the drop relative to the radius of the affected material surrounding the drop.

E. Friction changes

Measurements of the lateral deflection of the cantilever show significant differences between the material in the pits and the surrounding material. Figure 10(a) shows a topographic image of representative pits. Figure 10(b) was formed by plotting the difference between the lateral force measured as the AFM tip passes from left to right and the lateral force measured as the tip passes from right to left. This difference reflects the frictional force experienced by the tip during scanning. Many of the pits in the lateral force difference image of Fig. 10(b) show well-defined rings that reflect the transient change in lateral force as the tip passes over the pit rims. However, the contrast between the pit bottoms and the surrounding material reflects differences in frictional behavior. Darker regions correspond to lower friction. In Fig. 10(b), the apparent friction along the bottom of these pits is about 20% lower than the apparent friction well outside the pits. The reduced friction is consistent with the harder, stiffer material along the bottom of the pit. Similar measurements on a number of pits show drops of 10%–60% in apparent friction as the tip crosses the pit.

IV b. DISCUSSION

A. Pit formation

We attribute pit formation to the local densification of polymer in contact with drops of condensed formic acid. Because localized solvent treatments typically swell polymers,[17] we expect that condensed formic acid initially diffuses into the PMMA to produce a bump. For instance, we have produced bumps on PMMA by small area scanning at modest contact forces in weak solvents, including dilute ethanol solutions.[18] Weak solvents require mechanical stimulation by the atomic force microscope tip for significant solvent uptake in the PMMA.

Formic acid diffuses rapidly even in the absence of mechanical stimulation, and would swell any PMMA in contact with the drop.

Formic acid readily attacks PMMA. The formate ion is chemically similar to the carbomethoxy side group of PMMA, which plays a major role in the PMMA glass transition. Interactions between the carbomethoxy side group and formic acid molecules would induce sidegroup motions that open up voids for the formic acid molecule, allowing for rapid diffusion into the bulk. These motions are similar to those responsible for the rubber-like behavior of PMMA at temperatures above the T_g. PMMA soaks up formic acid like a sponge and swells accordingly.

An unexpected observation in this work is the net negative volume change associated with most pits. For instance, Bonaccurso et al.[7] measured a net positive volume change associated with pits produced by toluene on polystyrene. The density and mechanical properties of cast films depend strongly on the solvent.[19] Fu et al.[20] demonstrated significant density differences in PMMA films cast in six good solvents. For instance, films cast from dichloromethane (boiling point, $T_b \approx 40$ °C) were denser than films cast from methyl isobutyl ketone ($T_b \approx 115$ °C). Although several solvent properties contribute to the film density, the most important solvent property in this comparison was solvent volatility. Fu et al.[20] attributed the high density of films cast in low-T_b solvents to rapid solvent diffusion and evaporation, which can hinder the random chain coiling responsible for low-density films. Formic acid ($T_b \approx 101$ °C) is much more volatile than the solvents used to cast our films (propylene glycol methyl ether acetate, $T_b \approx 145$ °C; γ-butyrolactone, $T_b \approx 204$ °C), which is consistent with film densification. The very small size of the formic acid molecule also promotes especially rapid diffusion, further favoring densification.

Assuming that the densified polymer occupies a hemisphere with a diameter equal to the pit diameter, a density increase of ≈1% is required to account for the observed net volume change. Density increases of 1%–2% are readily achieved by annealing PMMA films.[21] The density increase is supported by nanoindentation measurements of hardness and stiffness along the pit bottoms; denser material is normally harder and stiffer, as observed. Harder polymers also typically display lower friction than softer polymers, consistent with the lower friction observed along the pit bottoms. Because we can form pits in films annealed for 2 h at 140 °C, it appears that formic acid has a greater effect on polymer density than modest annealing treatments.

The effect of solvent-induced densification on pit depths clearly depends on how deep the solvent penetrates into the polymer (the volume of affected material), which increases with longer exposure times and larger drops. If high evaporation rates are required for densification, one expects that excessive exposure times will reduce pits depths. We expect that long formic acid exposures also promote wetting of the PMMA surface; as formic acid diffuses radially outward from a drop, parallel to the surface, the surrounding PMMA will become saturated with acid and promote wetting by the liquid. The drops would then spread laterally. This is consistent with the broad, shallow pits formed by long formic acid exposures. The optimum acid exposure will be a compromise between the need to allow for sufficient diffusion downward into the bulk, and the need to minimize lateral diffusion.

Polymer densification accounts for about 75% of the volume of typical pits in this work. Densification is responsible for most of the pit depth, and is therefore largely responsible for the high-aspect-ratio pits in this work (depth-to-diameter ratio up to 0.5). In the absence of densification, the aspect ratios of the pits in this work would likely be similar to those produced by Bonaccurso et al.[7] on polystyrene, where densification was not observed.

B. Rim formation

Bonaccurso et al.[7] produced pits 15–150 μm in diameter by depositing toluene drops on polystyrene surfaces. They attribute pit and rim formation to the "coffee stain effect," where enhanced evaporation along the drop perimeter[22] drives the transport of suspended solids to the perimeter, where it is deposited.[4] This mechanism is responsible for the brown, ring-like deposits formed when coffee is spilled on a hard surface.

The pits formed on PMMA by formic acid drops are much smaller, suggesting that other processes are important. On submicron scales, for instance, material transport by diffusion often dominates over convection. Further, the dissolution of long polymer chains in small solvent volumes can become difficult. Stretched end to end, an average polymer chain in this work (MW ≈ 145k) is about 400 nm long. Freeing a chain this long from a solid and dissolving it in a drop only 50 nm in diameter (the smallest drops observed in this work) does not seem likely.

We suggest that the rims are formed due to the radial expansion of swollen polymer toward the rim, followed by the early drying of material around the rim. As a formic acid drop diffuses into the PMMA, the surface will initially swell upward. As the free surface of the PMMA rises above the surrounding surface, hydrostatic pressure in the swollen material will displace some material radially outward, toward the perimeter of the drop. Later, this material will lose its solvent first due to the low solvent concentration in the polymer surrounding the drop. This material will then be frozen in its displaced state before the interior of the pit dries. The displaced material would form a rim around the perimeter of the pit and leave a depression near the center, consistent with observations. In cases where solvent removal is more uniform,

rims would not be formed. This would account for the lack of rims on some of the pits described above. In the current work, rim formation typically adds 25% to the pit volume, without contributing much to the pit area.

Given sufficient pit densities, these rims have the potential to reduce the surface wetability by minimizing the area of contact between the surface and adhering water drops. For instance, water drops on lotus leaves are supported away from the surface on nanometer-scale projections; these drops are easily removed from the leaf and often take dust particles with them when they leave. Thus, lotus leaves are said to be "self-cleaning." Self cleaning nanostructured surfaces would have important applications if they can be manufactured economically.

C. Effect of ammonia vapor

Relatively short exposures to formic acid vapor yield deeper pits when followed immediately by exposure to room-temperature ammonia vapor. We attribute this effect to the effect of ammonia on the surface tension of the formic acid drops. Although adding either ammonia or formic acid to water typically decreases surface tension, adding both (the salt) increases surface tension.[23] Thus, one effect of ammonia exposure would be to briefly neutralize formic acid near the surface of a drop, increasing the surface tension and contact angle. Decreasing the drop radius and increasing its thickness would favor deeper diffusion of formic acid into the PMMA, which would increase the thickness of the densified material and increase the pit depth.

D. Effect of acid concentration

The concentration of formic acid in the solution used to provide vapor also influences the size and depth of the resulting pits. Decreasing the concentration of formic acid in the source liquid should decrease the vapor pressure of formic acid above the bath and decrease the concentration in formic acid in the condensed drops. Lower acid concentrations in the drops would increase surface tension, favoring drops with smaller areas and allowing deeper solvent penetration. However, water is a very poor solvent for PMMA; any water in the condensed drops would hinder the diffusion of formic acid into the bulk. Decreasing the formic acid concentration from 98% to 90% under the conditions used in Fig. 7 increases the pit depth.

As the formic acid concentration is further reduced to 80% in Fig. 8, the diameters of the largest pits grow significantly. At this concentration, the evaporation is increased to the point where diffusion promotes localized wetting. The resulting pits tend to be broad and shallow. A similar effect is observed when the duration of formic acid exposure is increased to long times (Fig. 6). Under these conditions, the deepest pits were formed by condensation of over 90% formic acid.

E. Control of drop size distribution

Although the nucleation and growth of formic acid drops was not directly observed in this work, the size, shape, and lifetime of the resulting drops determines the size and shape of the resulting pits. Some pits show evidence for complicated drop histories, including the large pit seen in Fig. 3 and the flower-like pit seen in Fig. 4(a). Strategies for controlling initial drop

densities and subsequent growth are expected to have comparable effects on pit density, size, and geometry.

Drops produced by condensation can be very small. A drop with the diameter of the pit seen in Fig. 2 and a contact angle of 25° would have a volume of 3×10^{-15} L. This is <1% of the drop volume in a typical ink-jet printer (2×10^{-12} L). Significantly, smaller pits with similar geometries can be obtained with shorter solvent exposures: the smallest pits observed were 50 nm in diameter. This measurement is actually limited by the tip radius.

Condensation also allows for the use of especially volatile, reactive solvents, like formic acid. High volatility allows for rapid evaporation and thus short contact times. Although rapid evaporation reduces the time available for solvent diffusion into the film, it also minimizes diffusion parallel to the surface, which increases the pit diameter. Thus, especially volatile solvents are likely to yield the smallest (diameter) pits.

The solvent volume applied per unit drop area can be maximized by choosing solvents with high surface tensions, which allow for drops with high contact angles. High contact angles promote solvent diffusion into the film (and thus pit depth), while minimizing radial diffusion parallel to the surface (and thus pit diameter). Thus, increasing the solvent surface tension would favor the formation of pits with high aspect ratios. This may be especially important for very small pits; drops smaller than a micrometer in diameter often display reduced contact angles due to unavoidable surface heterogeneities.[24]

Significantly, the surface tension of 90% formic acid (41 mN/m) is considerably higher than the surface tension of pure toluene (28 mN/m),[25] which is used successfully to produce much larger pits on polystyrene films. The relatively low surface tension of toluene may have

contributed to the relatively low aspect ratios of these pits (< 0.1).[7] Unfortunately, producing small drops of high-surface-tension fluids by flow through an orifice can be difficult. In addition, high-surface-tension drops often display poor adhesion to many surfaces. These difficulties can be circumvented by condensing the solvent onto the surface.

To modify surface properties, a high density of relatively small, uniform structures is often desired. Given sufficient drop-nucleation densities, high-surface-energy solvents on low-surface-energy surfaces (like PMMA) can produce high densities of relatively uniform drops if exposure is terminated just before the drops become large enough to touch and coalesce. Immediately prior to the onset of coalescence, surface coverages as high as 55% can be reached,[26] which corresponds to the limiting surface coverage for randomly packed, uniform disks.[27] Choosing solvent vapor pressures and exposure times to maximize drop size but avoid coalescence would be a useful strategy for optimizing pit uniformity while maintaining relatively high coverage. Higher drop coverage is possible after coalescence, but the pit sizes are less uniform.

For some applications, the random distribution of pits formed by condensation is problematic. In microlens and microvessel arrays, pit location must be carefully controlled. It is possible that pit locations can be controlled to a large degree by manufacturing nucleation sites where pits are desired, perhaps using lithographic techniques. Currently, this control has not been demonstrated.

V. CONCLUSION

Large numbers of micron- and submicrometer diameter pits can be produced on PMMA films by briefly exposing them to formic acid vapor. Pit formation under these conditions is largely due to the densification of polymer surrounding the condensed acid drops. Nanoindentation measurements of hardness and stiffness support this mechanism. Many pits display raised rims. The size of drops formed by condensation can be much smaller than drops directly deposited on the surface. Highly volatile solvents are readily deposited by condensation, minimizing solvent contact time and the resulting pit areas. Both effects contribute to the small diameter and high aspect ratio of the pits observed in this work. The smallest pits in this work were about 50 nm in diameter, with a maximum aspect ratio (depth-to-diameter) of 0.5; both are significant improvements over previously reported pits, which were as small as 20 μm in diameter, with aspect ratios as high as 0.1.[7]

Drop nucleation and growth is relatively well understood. It is reasonable to expect that carefully controlled exposures to well-characterized vapors will result in high densities of even smaller pits with higher aspect ratios. Although the pit positions are random, we expect surface coverages as high as 55% can be obtained. Pitted films could also be used as templates for the casting of films with high bump densities. In some environments, these pits or the corresponding bumps would have a profound effect on the physical properties of the surface. Finally, controlled positioning of droplet nucleation might be possible using various nanolithographic tools such as particle-beam exposure. A number of such methods are under consideration.

ACKNOWLEDGMENTS

This work was supported by the National Science Foundation under Grants CMS-04-09861 and CHE-02- 34726, by the National Institutes of Health under Contract No. HG-002647-01A1, and by a Washington State University Center for Integrated Biotechnology Summer Research Grant. We thank Dr. David Bahr and Julie Reid, School of Mechanical and Materials Engineering at Washington State University for their assistance in the nanoindentation measurements.

REFERENCES

1. M.C. Wu: Micromachining for optical and optoelectronic systems. *Proc. IEEE* 85, 1833 (1997).
2. N.D. Denkov, O.D. Velev, P.A. Kralchevsky, I.B. Ivanov, H. Yoshimura, and K. Nagayama: Mechanism of formation of two-dimensional crystals from latex particles on substrates. *Langmuir* 8, 3183 (1992).
3. A.B. El Bediwi, W.J. Kulnis, Y. Luo, D. Woodland, and W.N. Unertl: Distributions of latex particles deposited for water suspensions, in *Hollow and Solid Spheres and Microspheres: Science and Technology Associated With Their Fabrication and Application*, edited by D.L. Wilcox, Sr., M. Berg, T. Bernat, D. Kellerman, and J.K. Cochran, Jr. (Mater Res. Soc. Symp Proc. 372, Pittsburgh, PA, 1995), p. 277.
4. R.D. Deegan, O. Bakajin, T.F. Dupont, G. Huber, S. Nagel, and T.A. Witten: Capillary flow as the cause of ring stains from dried liquid drops. *Nature* 389, 827 (1997).
5. P. Laden, editor: *Chemistry and Technology of Water Based Ink* (Blackie Academic, London, 1997).

6. G. Hanna and W.J.P. Barnes: Adhesion and detachment of the toe pads of tree frogs. *J. Exp. Biol.* 155, 103 (1991).
7. E. Bonaccurso, H-J. Butt, B. Hankeln, B. Niesenhaus, and K. Graf: Fabrication of microvessels and microlenses from polymers by solvent droplets. *Appl. Phys. Lett.* 86, 124101 (2005).
8. G. Li, H-J. Butt, and K. Graf: Microstructures by solvent drop evaporation on polymer surfaces: Dependence on molar mass. *Langmuir* 22, 11395 (2006).
9. G. Li, N. Höhn, and K. Graf: Microtopologies in polymer surfaces by solvent drop in contact and noncontact mode. *Appl. Phys. Lett.* 89, 241920 (2006).
10. S. Karabasheva, S. Baluschev, and K. Graf: Microstructurs on soluble polymer surface via drop deposition of solvent mixtures. *Appl. Phys. Lett.* 89, 031110 (2006).
11. F. Family and P. Meakin: Kinetics of droplet growth processes: Simulations, theory, and experiments. *Phys. Rev. A: At., Mol., Opt. Phys.* 40, 3836 (1989).
12. B.J. Briscoe and K.P. Galvin: An experimental study of the growth of breath figures. *Colloids Surf.* 56, 263 (1991).
13. P. Meakin: Droplet deposition growth and coalescence. *Rep. Prog. Phys.* 55, 157 (1992).
14. R. Williams and J. Blanc: Inhibition of water condensation by a soluble salt nucleus. *J. Chem. Phys.* 74, 4675 (1981).
15. R.N. Leach, F. Stevens, S.C. Langford, and J.T. Dickinson: Dropwise condensation: Experiments and simulations of nucleation and growth of water drops in a cooling system. *Langmuir* 22, 8864 (2006).
16. A.W. Adamson and A.P. Gast: *Physical Chemistry of Surfaces*, 6th ed. (Wiley, New York, 1997).

17. L.H. Sperling: *Physical Polymer Science*, 3rd ed. (John Wiley, New York, 2001).

18. R.N. Leach, F. Stevens, C. Seiler, S.C. Langford, and J.T. Dickinson: Nanometer-scale solvent-assisted modification of polymer surfaces using the atomic force microscope. *Langmuir* 19, 10225 (2003).

    A. Carre, D. Gamet, J. Schultz, and H.P. Schreiber: Nonuniformity in thin polymer films. *J. Macromol. Sci., Chem.* A23, 1 (1986).

19. Y-J. Fu, C-C. Hu, K-R. Lee, H-A. Tsai, R-C. Ruaan, and J-Y. Lai: The correlation between free volume and gas separation properties in high molecular weight poly(methyl methacrylate) membranes. *Eur. Polym. J.* 43, 959 (2007).

20. H. Richardson, C. Carelli, J.L. Keddie, and M. Sferrazza: Structural relaxation of spin-case polymer thin films as a possible factor in dewetting. *Eur. Phys. J., E: Soft Matter* 12, 437 (2003).

21. J. Israelachvili: *Intermolecular and Surface Forces* (Academic Press, New York, 1992).

22. W.J. Moore: *Physical Chemistry* (Prentice Hall, Englewood Cliffs, NJ, 1962).

    A. Checco, P. Guenoun, and J. Daillant: Nonlinear dependence of contact angle of nanodroplets on contact line curvature. *Phys. Rev. Lett.* 91, 186101 (2003).

23. Surface tension of aqueous mixtures, in *CRC Handbook Chemistry and Physics*, 85th ed., edited by D.R. Lide (CRC Press, Boca Raton, LA, 2004), p. 6.

24. B.J. Briscoe and K.P. Galvin: The evolution of a 2D constrained growth system of droplets: Breath figures. *J. Phys. D: Appl. Phys.* 23, 422 (1990).

25. M. Tanemura: On random complete packing by discs. *Ann. Inst. Statist. Math., B* 31, 351 (1979).

VI. APPENDIX

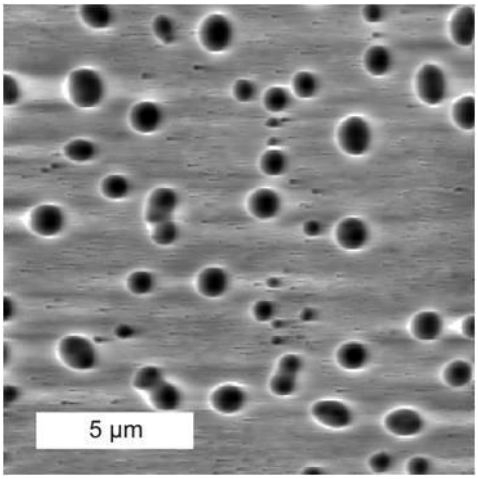

FIG. 1. A 20 × 20-µm2 AFM image of a PMMA film exposed to vapor from 98% formic acid at 65 °C for 5 s, followed by immediate exposure to ammonia vapor.

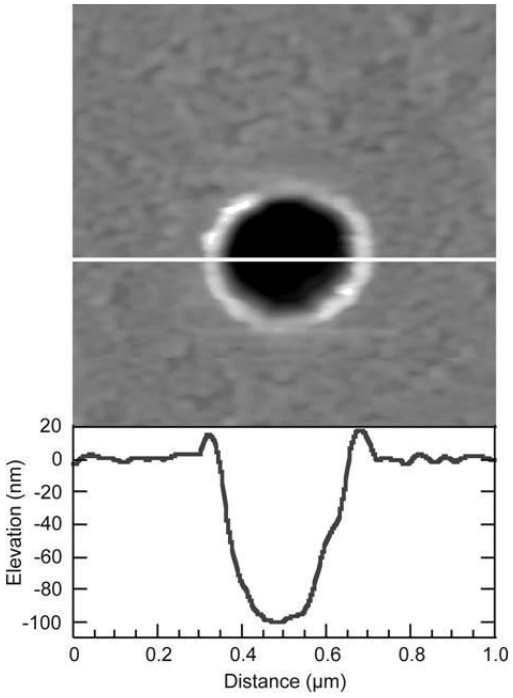

FIG. 2. Topographic image (above) and profile (below) of a pit formed by exposing a PMMA film to 70 °C, 98% formic acid for 3 s, followed by immediate exposure to ammonia vapor. The pit is approximately 300 nm in diameter and 100 nm deep.

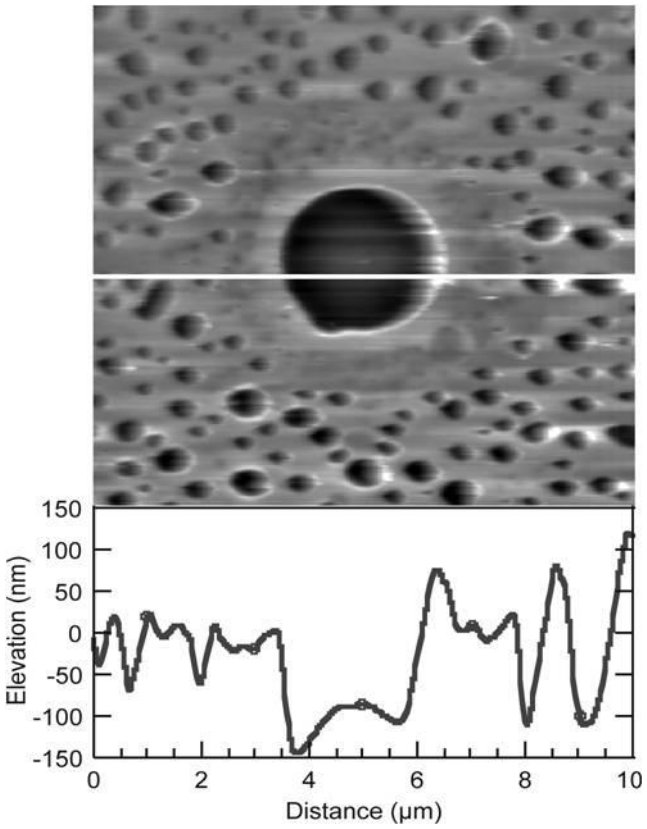

FIG. 3. Pits formed on a PMMA film exposed to 50 °C, 88% formic acid for 3 s, followed by immediate exposure to ammonia vapor. The largest pit has a raised bump in the center of the pit.

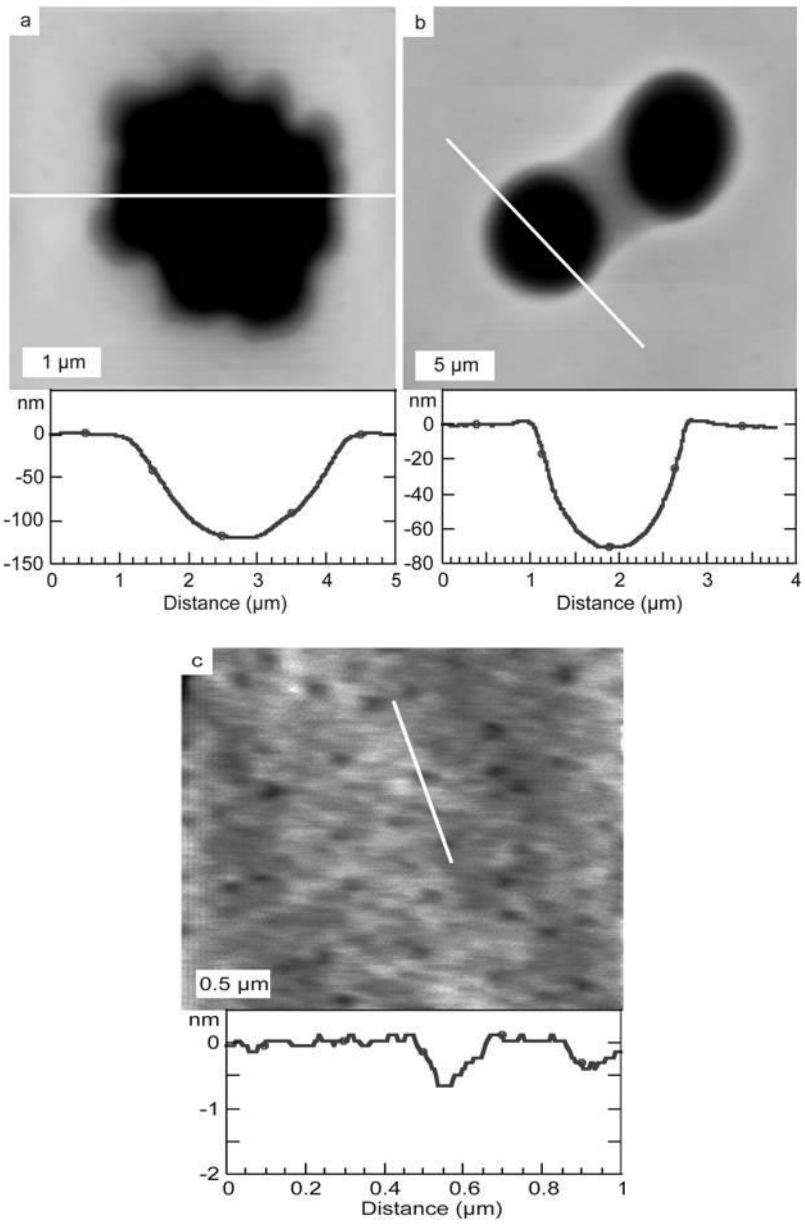

FIG. 4. (a) Flower-like pit on a PMMA film exposed to vapor from 60 °C, 88% formic acid for 5 s, without subsequent ammonia exposure. (b) Two deep, circular pits joined by a shallow neck, formed on a film exposed to vapor from 60 °C, 88% formic acid for 15 s without subsequent ammonia exposure. (c) Small, shallow, pit like features on a film exposed to vapor from 60 °C, 88% formic acid for 30 s without subsequent ammonia exposure.

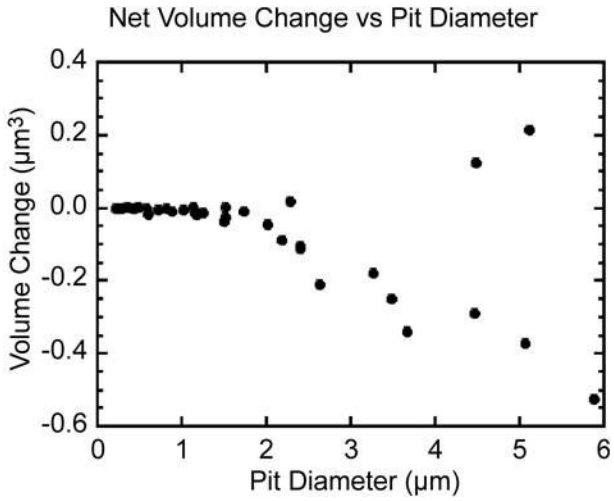

FIG. 5. Net volume change as a function of pit diameter for isolated pits formed using a variety of solvent concentrations, exposure times, and bath temperatures. The less common net-positive volume change consists of pits with much larger raised rims.

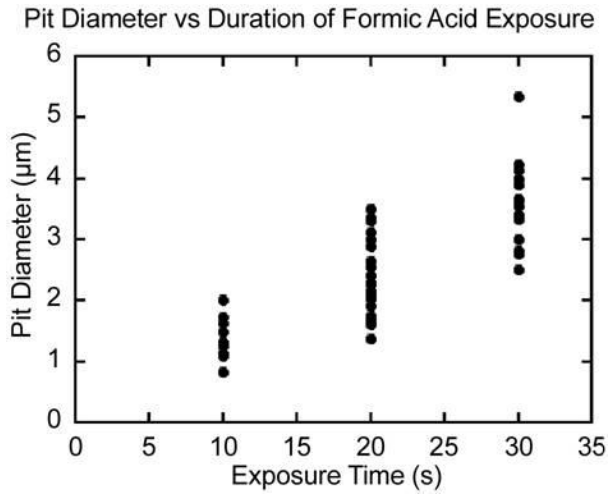

FIG. 6. Plot of pit diameters for films exposed to 50 °C, 98% formic acid as a function of exposure time, without subsequent ammonia exposure.

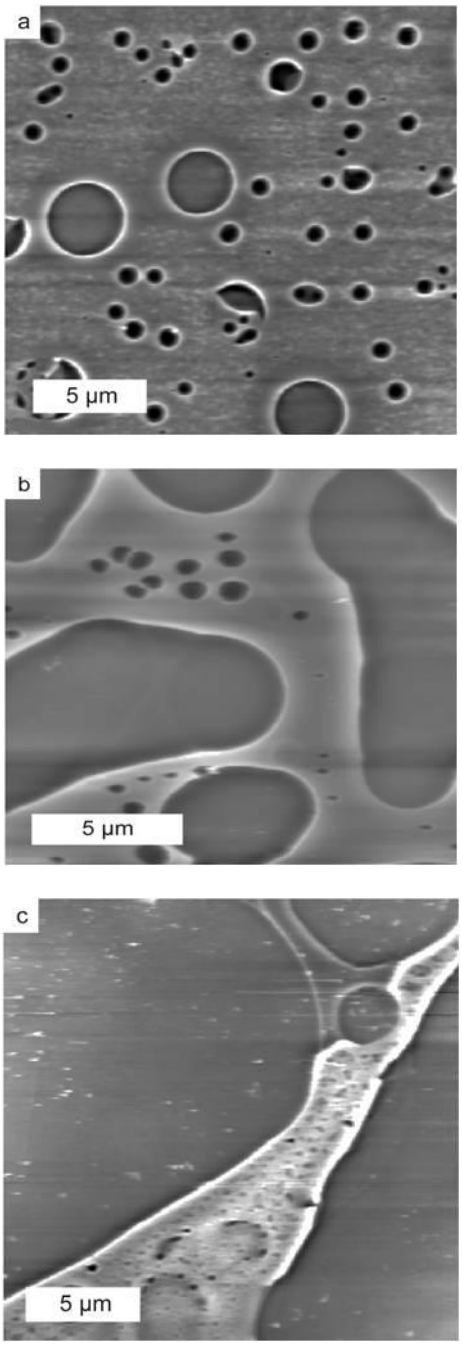

FIG. 7. PMMA films exposed to (a) 98%, (b) 90%, and (c) 80% formic acid at 65 °C for 5 s followed immediately by exposure to ammonia vapor.

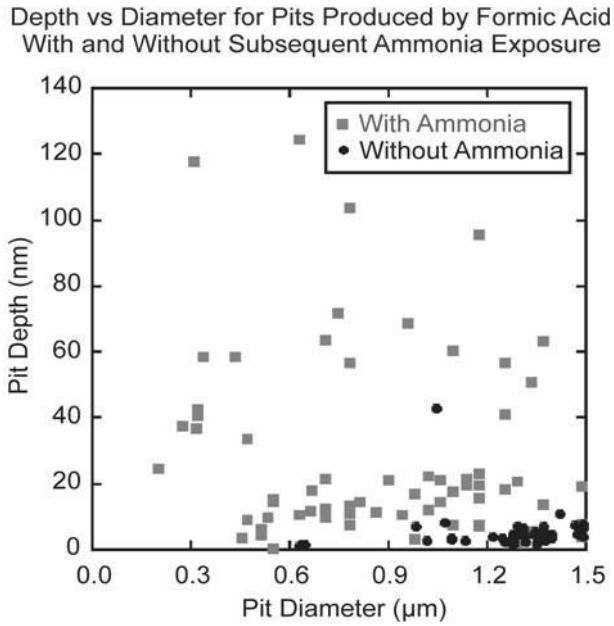

FIG. 8. Scatter plot of pit depths and diameters for films exposed to 98% formic acid, with and without subsequent ammonia exposure. The exposure duration and acid temperature were varied to yield a wide range of pit sizes.

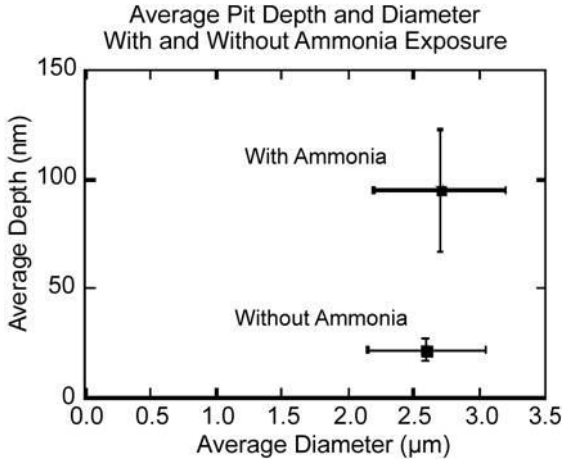

FIG. 9. Plot of average pit depth and diameter for pits formed by a 10-s exposure to 50 °C, 88% formic acid, with and without subsequent ammonia exposure. The error bars show the standard deviations of the depth and diameter measurements.

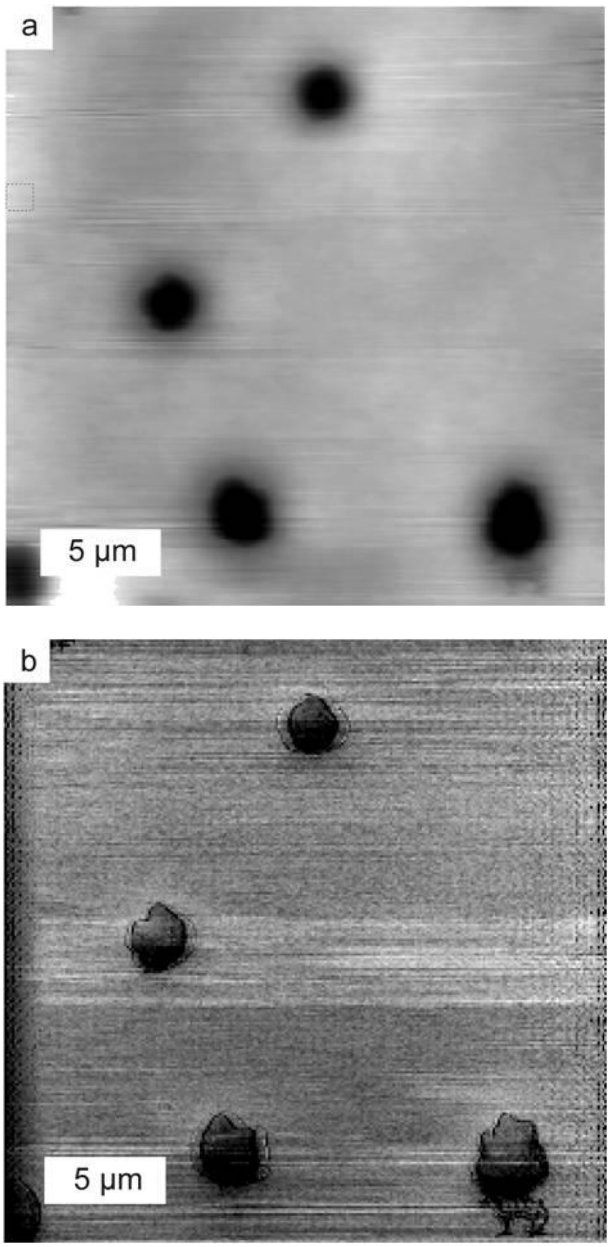

FIG. 10. (a) Topographic image of PMMA film exposed for 15 s to vapor from 98% formic acid heated to 50 °C (no ammonia exposure). (b) Lateral-force-difference image, formed by subtracting the lateral force measured as the tip moves from right to left from the lateral force measured as the tip moves from left to right. This difference is proportional to the frictional force. Regions with high friction appear bright, while regions with low friction appear dark. The applied normal force was 30 nN.